On the significance of reflection coefficients produced by active surfaces bounding one-dimensional sound fields

Timothy W. Leishman
Department of Physics and Astronomy, Brigham Young University, Eyring Science Center, Provo, Utah 84602

Jiri Tichy
Graduate Program in Acoustics, The Pennsylvania State University, Applied Science Building, University Park, Pennsylvania 16802

(Received 13 March 2001; revised 10 December 2002; accepted 13 December 2002)

Active boundary surfaces intended to control reverberation or other characteristics of enclosed sound fields have often been investigated using plane wave tubes. This paper presents an analysis of actively terminated semi-infinite and finite-length plane wave tubes to provide needed clarification of the effects of these surfaces. By considering relationships between complex pressure-amplitude reflection coefficients and acoustic energy quantities, the investigation reveals that increases in reflection coefficient moduli at terminations do not always produce corresponding increases in total energy or energy flux in adjacent fields. These relationships are shown to depend upon physical properties of the acoustic spaces, sources, and source positions. The investigation also demonstrates how the impact of reflection coefficients with moduli exceeding unity may be easily misinterpreted. © *2003 Acoustical Society of America.* [DOI: 10.1121/1.1550924]

PACS numbers: 43.50.Ki, 43.20.Tb, 43.20.Mv [MRS]

I. INTRODUCTION

The concept of utilizing active devices (e.g., electroacoustic transducers driven by electronic controllers) as acoustically responsive elements of enclosure boundaries has been investigated by many authors.[1–14] In contrast to elements of artificial reverberation systems, which attempt to recreate or synthesize desired acoustical signatures in rooms, these elements are intended to directly alter acoustical properties of enclosure boundaries or interact with primary sound sources to control specific sound field quantities.

Individual active boundary elements have frequently been evaluated as terminations to plane wave tubes.[3,5–9,11,14] Unfortunately, certain physical characteristics of these systems have been overlooked and capabilities of active boundary surfaces have consequently been misconstrued. In particular, complex pressure-amplitude reflection coefficients produced by active terminations and their relationships to acoustic energy quantities have been misunderstood, and implications of reflection coefficients with moduli exceeding unity ($|R|>1$) have largely been left to supposition. Because their characteristics are germane to extended enclosures with active boundary surfaces and fully three-dimensional fields, a concrete exploration of basic plane wave systems is important as a basis for further investigation.

One interpretation of $|R|>1$, from an exploration of active boundary elements, indicates that it connotes an increase in intensity in the adjacent field.[5] Another interpretation, from a study involving adaptive control of acoustic impedance, indicates that it connotes a supply of energy to the field.[8] (This notion agrees in part with the thinking of Morse and Ingard, who inauspiciously suggest that an active boundary surface ''feeds'' energy into an adjacent medium containing sources, independent of its reflection coefficient.[15]) A third interpretation, from a study of active surfaces intended for use in reverberant rooms, suggests that it connotes a super-reflection that increases reverberation in the field.[11] On the surface these interpretations may appear unobjectionable. However, further analysis reveals that they either inadequately or inaccurately characterize this attribute of active boundary surfaces—in both the plane wave tube arrangements used by their authors and in more general applications. They may have been based upon extrapolations from properties of passive materials, a hypothetical condition of constant incident pressure, or other preconceptions.

The problem of establishing effects of active boundary surfaces involves three interrelated facets. First, motion of an active boundary in the presence of impinging sound waves can produce a wide range of reflection coefficients, far greater than that of passive materials. Second, if another source exists in an adjacent finite space, vibration of an active boundary surface causes interactions with this source and consequently affects the field in a way that influences acoustic pressure incident upon itself—and its own reflection coefficient. Third, active boundary surfaces have acoustic impedances and reflection coefficients that are functions not only of their own vibrations, but vibrations of other sources within the adjacent space. Because these characteristics are not generally considered in the evaluation of common passive boundary materials, they are easily overlooked or misunderstood. Clearly, active boundary surfaces cannot be judged in the same context as passive boundary surfaces—particularly when their reflection coefficient moduli exceed unity.

To explore these matters further, this paper presents an analysis of two actively terminated plane wave tubes: a semi-infinite tube and a finite-length tube. Each incorporates a uniformly vibrating cross-sectional piston as an active

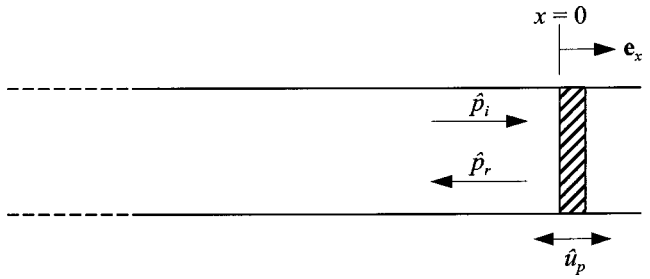

FIG. 1. Active vibrating piston terminating a semi-infinite plane wave tube. Constant incident pressure plane waves impinge upon the piston from a hypothetical source located at infinite distance to the left.

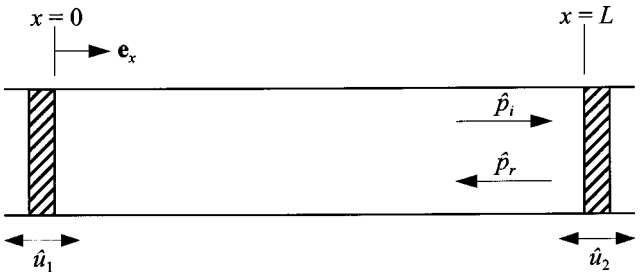

FIG. 2. Finite-length plane wave tube with active vibrating pistons at either end. The system behaves as an impedance tube driven by a primary source (piston 1) and terminated by an active boundary surface (piston 2).

boundary surface. Various sound field quantities are derived and relationships between their reflection coefficients and certain energy-related acoustic quantities are carefully examined. A few previously investigated aspects of the systems are briefly summarized in the analysis because of their pertinence.

II. ACTIVE PISTON TERMINATING A SEMI-INFINITE PLANE WAVE TUBE

Figure 1 depicts a lossless semi-infinite plane wave tube of cross-sectional area S terminated by an active uniformly vibrating piston. The piston vibrates freely but snugly with velocity $\mathbf{u}_p(t)=\mathrm{Re}\{\hat{u}_p \exp(j\omega t)\}\mathbf{e}_x$ inside the end of the tube.[16] This arrangement yields a convenient condition of constant incident pressure on the piston while precluding the need to address acoustic interaction with a primary source. The piston oscillates at the same angular frequency ($\omega = 2\pi f$) as the plane wave incident from the left, which is lower than the cutoff frequency of the first tube cross mode. The characteristic fluid impedance in the tube is $\rho_0 c$, where ρ_0 is the ambient fluid density and c is the speed of sound.

The specific acoustic impedance and pressure–amplitude reflection coefficient posed to the sound field by the vibrating piston may be represented as

$$Z_S=\frac{\hat{p}_B}{\hat{u}_p}-\rho_0 c \tag{1}$$

and

$$R=1-\rho_0 c\frac{\hat{u}_p}{\hat{p}_i}, \tag{2}$$

where $\hat{p}_B=2\hat{p}_i$ is the blocked surface pressure on the piston face. The piston velocity accordingly controls both the impedance and the degree of sound reflection, easily producing values of $|R|>1$.

Active acoustic intensity I in the tube may be expressed in terms of incident and reflected intensities or equivalently in terms of the incident intensity and the reflection coefficient:[17]

$$I=I_i-I_r=I_i(1-|R|^2). \tag{3}$$

Total time-averaged energy density w, with potential and kinetic energy density components, may likewise be expressed using the reflection coefficient:

$$w=w_p+w_k=\frac{|\hat{p}_i|^2}{2\rho_0 c^2}(1+|R|^2)=\frac{I_i}{c}(1+|R|^2). \tag{4}$$

The intensity, the related sound power, and the energy density are all independent of distance from the piston.

III. ACTIVE PISTON TERMINATING A FINITE-LENGTH PLANE WAVE TUBE

A lossless finite-length tube with uniformly vibrating pistons at either end extends the analysis of the active boundary surface to include its interaction with another source and a completely enclosed sound field. Although this model has been used elsewhere for analytical studies,[18–23] it is used here with a different emphasis. Figure 2 depicts the system, which involves a tube of length L and cross-sectional area S. The termination is controlled to respond in various ways to the primary source. If the velocities of the two pistons are known, several interesting aspects of the system may be considered, including basic acoustic quantities and sound field control.

A. Basic acoustic quantities

If pistons 1 (left) and 2 (right) vibrate with velocities $\mathbf{u}_1(t)=\mathrm{Re}\{\hat{u}_1 \exp(j\omega t)\}\mathbf{e}_x$ and $\mathbf{u}_2(t)=-\mathrm{Re}\{\hat{u}_2 \times \exp(j\omega t)\}\mathbf{e}_x$, respectively,[24] the boundary conditions yield the following relationships for acoustic pressure and particle velocity:

$$\hat{p}(x)=-j\rho_0 c\hat{u}_1\left[\sin kx+\left(\cot kL+\frac{\hat{u}_2}{\hat{u}_1}\csc kL\right)\cos kx\right], \tag{5}$$

$$\hat{\mathbf{u}}(x)=\hat{u}_1\left[\cos kx-\left(\cot kL+\frac{\hat{u}_2}{\hat{u}_1}\csc kL\right)\sin kx\right]\mathbf{e}_x \tag{6}$$

or

$$\hat{p}(x)=\frac{-j\rho_0 c}{2\sin kL}[(\hat{u}_1 e^{jkL}+\hat{u}_2)e^{-jkx}+(\hat{u}_1 e^{-jkL}+\hat{u}_2)e^{jkx}], \tag{7}$$

$$\hat{\mathbf{u}}(x)=\frac{-j}{2\sin kL}[(\hat{u}_1 e^{jkL}+\hat{u}_2)e^{-jkx} -(\hat{u}_1 e^{-jkL}+\hat{u}_2)e^{jkx}]\mathbf{e}_x, \tag{8}$$

where $k=\omega/c$ is the acoustic wave number. These results may be used to show that the specific acoustic impedance posed to the field by the active termination (piston 2) depends not only upon its own velocity, but upon the velocity of the primary source (piston 1):

$$Z_{S,2}=j\rho_0 c\left(\cot kL+\frac{\hat{u}_1}{\hat{u}_2}\csc kL\right) \tag{9}$$

(compare Ref. 22).

The reflection coefficient at $x=L$ may be obtained in a straightforward manner from this impedance or by using Eq. (7) with the relationship $R=\hat{p}_r/\hat{p}_i$:

$$R|_{x=L}=\frac{\hat{u}_1+\hat{u}_2 e^{jkL}}{\hat{u}_1+\hat{u}_2 e^{-jkL}}. \tag{10}$$

Because R also depends upon both $\hat{u}_1$ and $\hat{u}_2$, one may modify its value to achieve a desired degree of reflection or absorption at the termination by adjusting *either* piston velocity. For example, if total absorption $(R=0+j0)$ is required, the velocity condition is simply $\hat{u}_2=-\hat{u}_1 \times\exp(-jkL)$.[20,21] If R is constrained in this fashion, the condition eliminates steady-state pressure reflected from the termination. Steady-state pressure *incident* upon the termination is eliminated if the velocities satisfy the condition $\hat{u}_2 =-\hat{u}_1\exp(jkL)$.

Equations (5)–(8) also lead to a relationship for intensity. The components incident upon and reflected from the active termination are

$$I_i=\frac{\rho_0 c}{8\sin^2 kL}|\hat{u}_1+\hat{u}_2 e^{-jkL}|^2, \tag{11}$$

$$I_r=\frac{\rho_0 c}{8\sin^2 kL}|\hat{u}_1+\hat{u}_2 e^{jkL}|^2 \tag{12}$$

which satisfy the relationship $I_r/I_i=|R|^2_{x=L}$. The total intensity is

$$\begin{aligned} I=I_i-I_r&=\frac{\rho_0 c}{2\sin kL}|\hat{u}_1|^2\ \mathrm{Im}\left\{\frac{\hat{u}_2}{\hat{u}_1}\right\}\\ &=\frac{\rho_0 c}{2\sin kL}(u_{1,I}u_{2,R}-u_{1,R}u_{2,I}), \end{aligned} \tag{13}$$

where the subscripts R and I denote real and imaginary components, respectively. Notably, each of these intensity expressions depends upon both piston velocities and is independent of position x. However, total intensity is nonzero only if *both* piston velocities are nonzero and the velocity ratio $\hat{u}_2/\hat{u}_1$ has an imaginary component. The corresponding sound power quantities, related by the tube cross-sectional area S, behave similarly.

Energy density in the tube is given by the expression

$$\begin{aligned} w&=w_p+w_k\\ &=\frac{|\hat{p}(x)|^2}{4\rho_0 c^2}+\frac{\rho_0|\hat{u}(x)|^2}{4}\\ &=\frac{\rho_0}{4\sin^2 kL}[|\hat{u}_1|^2+|\hat{u}_2|^2+2(u_{1,R}u_{2,R}\\ &\quad+u_{1,I}u_{2,I})\cos kL]. \end{aligned} \tag{14}$$

Because of its spatial uniformity, total acoustic energy in the tube is simply

$$\begin{aligned} E=E_p+E_k=\frac{\rho_0 SL}{4\sin^2 kL}&[|\hat{u}_1|^2+|\hat{u}_2|^2\\ &+2(u_{1,R}u_{2,R}+u_{1,I}u_{2,I})\cos kL]. \end{aligned} \tag{15}$$

Another quantity of special interest is the potential energy component of total energy

$$\begin{aligned} E_p&=S\int_0^L\frac{|\hat{p}(x)|^2}{4\rho_0 c^2}dx\\ &=\frac{\rho_0 SL}{8\sin^2 kL}\Bigg[(|\hat{u}_1|^2+|\hat{u}_2|^2)\\ &\quad\times\left(\cos kL\frac{\sin kL}{kL}+1\right)+2(u_{1,R}u_{2,R}+u_{1,I}u_{2,I})\\ &\quad\times\left(\cos kL+\frac{\sin kL}{kL}\right)\Bigg]. \end{aligned} \tag{16}$$

B. Sound field control

Because active boundary surfaces may be used to control specific sound field quantities,[21,25] a few pertinent examples are discussed here as a basis for later discussion of how these control schemes relate to termination reflection coefficients. To minimize total pressure at a position x in the tube, the required relationship between $\hat{u}_1$ and $\hat{u}_2$ may be determined by setting $\hat{p}(x)=0$ in Eq. (5):

$$\hat{u}_2=-\hat{u}_1(\tan kx\ \sin kL+\cos kL). \tag{17}$$

At very low frequencies, this relationship produces substantial pressure reduction throughout the entire tube, but at higher frequencies it can lead to pressure increases at other positions. A more useful objective might then be to achieve consistent *global* control of the field. A common approach to this problem for enclosed fields involves the minimization of total potential energy E_p.[21] Another advantageous approach is to minimize total energy density w at discrete positions.[26,27]

Given a fixed velocity $\hat{u}_1$, the total potential energy in the enclosure is minimized by the termination piston velocity

$$\hat{u}_2=-\hat{u}_1\left(\frac{\cos kL+\sin kL/kL}{\cos kL\sin kL/kL+1}\right) \tag{18}$$

(compare Ref. 20). The velocity required to minimize total energy density at any point within the enclosure is

$$\hat{u}_2 = -\hat{u}_1 \cos kL \tag{19}$$

which is the same as that required to control total energy E within the tube.[20,21] The solutions to control E_p and w converge when $kL \to n\pi$, where n is a non-negative integer, and more generally when $kL \gg \pi$. Several other energy control schemes could also be investigated using the model.[14]

IV. ENERGY-RELATED EFFECTS OF REFLECTION COEFFICIENTS PRODUCED BY ACTIVE TERMINATIONS

Having considered several fundamental characteristics of active terminations and adjacent plane wave tube sound fields, the discussion now turns to the central focus of the paper: the significance of reflection coefficients generated by these active surfaces. The preceding sections have demonstrated that reflection coefficient moduli of active boundary surfaces can easily exceed unity (i.e., $|R|>1$), the common upper bound for passive materials. On the other hand, they can easily replicate moduli of passive materials (i.e., $0 \leqslant |R| \leqslant 1$). This section interprets this wide range of reflection coefficients and its relationships to acoustic energy quantities in adjacent fields. It also reviews the past interpretations of $|R|>1$, demonstrating how their seemingly intuitive descriptions can be misleading.

A. Semi-infinite tube

When a piston terminating a semi-infinite tube (Fig. 1) is controlled to produce a reflection coefficient modulus of $|R|=0$, it produces no reflected intensity. From Eq. (3), it is clear that the total intensity becomes $I=I_i$ and from Eq. (4), the energy density becomes $w=I_i/c$. In contrast, when the piston is controlled to produce a reflection coefficient modulus of $|R|=1$, the reflected intensity magnitude equals the incident intensity magnitude ($I_r=I_i$), so from Eq. (3) the total intensity vanishes. From Eq. (4), the total energy density becomes double that present under the prior condition, i.e., $w=2I_i/c$. Thus, in comparison to an anechoic condition ($R=0+j0$), the imposition of a rigid termination ($R=1+j0$) increases energy in the field. Yet it simultaneously eliminates total sound-energy flux. This simple example demonstrates an important point: when one discusses boundary surfaces and their energy-related effects in an adjacent space, one must explicitly state both the specific energy quantity being considered and a comparative boundary condition. Because the two extreme passive conditions mentioned here provide useful benchmarks to compare active boundary surfaces, energy *ratios* that involve them are quite useful. Specifically, ratios of total intensity, reflected intensity, and total energy density (with arbitrary R) to the respective quantities determined under anechoic or rigid termination conditions merit consideration.

The useful intensity ratios for the semi-infinite tube are total intensity to that present under the anechoic condition and reflected intensity to that present under the rigid condition

$$\frac{I}{I_{an}} = 1 - |R|^2, \tag{20}$$

$$\frac{I_r}{I_{r,rg}} = |R|^2. \tag{21}$$

The ratios involving total energy density are

$$\frac{w}{w_{an}} = 1 + |R|^2, \tag{22}$$

$$\frac{w}{w_{rg}} = \frac{1}{2}(1 + |R|^2). \tag{23}$$

A number of conclusions may be drawn from these simple expressions and the related expressions of Sec. II. First, when $0<|R|<1$, total intensity remains positive. Sound-energy flux is directed toward the termination so that the piston absorbs at least a portion of the incident energy. Energy density in the field is greater than in the purely anechoic case, but less than in the purely rigid case. When $|R|>1$, the reflected intensity magnitude exceeds the fixed incident intensity magnitude and therefore the reflected intensity magnitude encountered under the rigid boundary condition. Total intensity becomes negative so sound-energy flux is directed away from the piston into the adjacent space. Both the vector magnitude of the total intensity and the energy density become greater than in either the anechoic or rigid case, growing in proportion to $|R|^2$. The active boundary with $|R|>1$ therefore *increases* both energy flow back to the field and total energy per unit tube length.

The past interpretations for $|R|>1$ mentioned in the introduction coincide well with this model and follow trends of passive materials. The first interpretation suggests that large reflection coefficient moduli create an increase in intensity. Its authors specifically indicate that $|R|>1.5$ provides "more than [a] doubling [of] acoustic intensity."[5] Significantly, this assertion appears plausible only if the indicated intensity refers to reflected intensity relative to that present under a rigid boundary condition [see Eq. (21)] or relative to incident intensity (from $I_r/I_i=|R|^2_{x=L}$). The second and third interpretations are also plausible. Nevertheless, the following section reveals deficiencies of the interpretations under more general conditions.

B. Finite-length plane wave tube

Energy-related quantities and ratios for the two-piston plane wave tube model (Fig. 2) may also be expressed in terms of the active termination reflection coefficient. However, a few general characteristics of the reflection coefficient modulus $|R|_{x=L}$ should first be considered.[28] As shown in Eq. (10), the complex reflection coefficient is a function of both the primary and secondary piston velocities. Its modulus may be expressed in terms of the complex velocity ratio $\hat{u}_2/\hat{u}_1$:

$$|R|_{x=L} = \left(\frac{1 + (\hat{u}_2^*/\hat{u}_1^*)e^{-jkL} + (\hat{u}_2/\hat{u}_1)e^{jkL} + |\hat{u}_2/\hat{u}_1|^2}{1 + (\hat{u}_2^*/\hat{u}_1^*)e^{jkL} + (\hat{u}_2/\hat{u}_1)e^{-jkL} + |\hat{u}_2/\hat{u}_1|^2} \right)^{1/2}. \tag{24}$$

From this relationship, it can be demonstrated that $\hat{u}_2/\hat{u}_1$ must have an imaginary component as a necessary condition for $|R|_{x=L} \neq 1$. This result is reminiscent of the condition for

nonzero active intensity discussed in Sec. III A. Interestingly, as demonstrated in Sec. III B, there are many control conditions that simply do not satisfy this requirement. For example, whether one controls acoustic pressure at a point, energy density, total energy, or total potential energy, the resulting reflection coefficient modulus remains the same: $|R|_{x=L}=1$.

Total intensity in the tube, expressed in terms of the termination reflection coefficient, is obtained from Eqs. (10) and (13):

$$I=\frac{\rho_0 c}{2}|\hat{u}_1|^2\left\{\frac{1-|R|^2_{x=L}}{|R|^2_{x=L}+1-2[(R_R|_{x=L})\cos 2kL+(R_I|_{x=L})\sin 2kL]}\right\}. \tag{25}$$

As with the semi-infinite tube, the useful intensity ratios are total intensity to that present under the anechoic condition and reflected intensity to that present under the rigid condition:

$$\frac{I}{I_{an}}=\frac{1-|R|^2_{x=L}}{|R|^2_{x=L}+1-2[(R_R|_{x=L})\cos 2kL+(R_I|_{x=L})\sin 2kL]}, \tag{26}$$

$$\frac{I_r}{I_{r,rg}}=\frac{4|R|^2_{x=L}\sin^2 kL}{|R|^2_{x=L}+1-2[(R_R|_{x=L})\cos 2kL+(R_I|_{x=L})\sin 2kL]}. \tag{27}$$

These expressions demonstrate that in the limit of large $R|_{x=L}$, i.e., $|R|_{x=L}\gg 1$, the ratio $I/I_{an}\rightarrow -1$ while the ratio $I_r/I_{r,rg}\rightarrow 4\sin^2 kL$. These results are important departures from the analogous results for the semi-infinite plane wave tube. Total intensity magnitude approaches that encountered under the *anechoic* boundary condition, but its sense is reversed (i.e., sound-energy flux is directed away from the termination and toward the enclosure and primary piston). Reflected intensity differs by a frequency-dependent factor $4\sin^2 kL$ when compared to that present under the rigid boundary condition.

Figure 3 shows a surface plot of I/I_{an} as a function of $R_R|_{x=L}$ and $R_I|_{x=L}$ for the frequency $f=9c/16L$. The rise between consecutive contour lines represents a ratio increment of 0.1. As the plot indicates, the ratio diverges both positively and negatively on either side of a single point on the complex $R|_{x=L}$ plane. At several other points, including those for which $|R|_{x=L}\gg 1$, it approaches a value of -1, as evidenced by the superposed mesh representing the $I/I_{an}=-1$ plane. (The divergences are truncated in the figure to focus attention on the behavior of the ratio near this plane.) Figure 4 provides additional insight through a closer overhead view of the contours. The heavy dashed circle indicates the values for which $|R|_{x=L}=1$. Notably, the eccentric contour rings become progressively smaller and closer together in the divergent regions with centers gradually approaching a

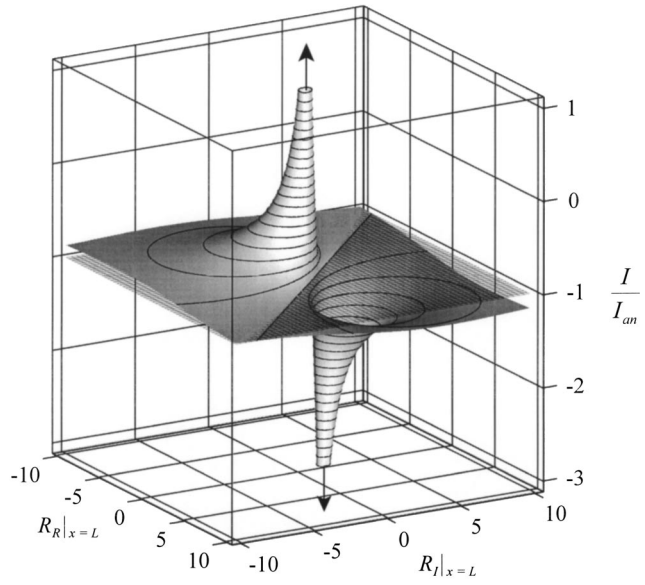

FIG. 3. Surface plot showing the ratio of total intensity in the two-piston plane wave tube to that present under an anechoic termination condition. The ratio is plotted as a function of the real and imaginary parts of the termination reflection coefficient, $R_R|_{x=L}$ and $R_I|_{x=L}$, for the frequency $f=9c/16L$. Contour lines are shown at increments of 0.1. The superposed mesh represents the $I/I_{an}=-1$ plane.

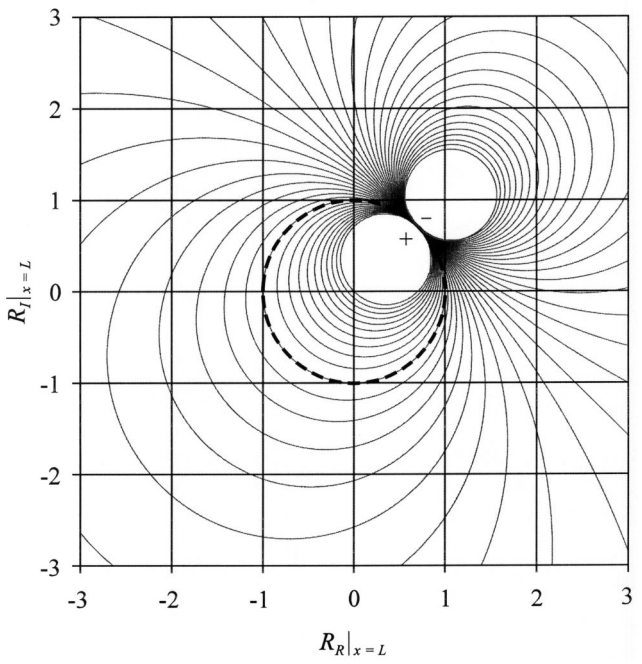

FIG. 4. Contour plot showing the ratio of total intensity in the two-piston plane wave tube to that present under an anechoic termination condition. The ratio is plotted as a function of the real and imaginary parts of the termination reflection coefficient, $R_R|_{x=L}$ and $R_I|_{x=L}$, for $f=9c/16L$. Contour lines are shown at increments of 0.1 with truncation at $I/I_{an}=1$ and -3 (see Fig. 3). The heavy dashed circle delineates $|R|_{x=L}=1$.

single point on this unit circle. Rings accumulating inside the circle correspond to the positive divergence, whereas those accumulating outside the circle correspond to the negative divergence. The series of rings are truncated at $I/I_{an}=1$ and $I/I_{an}=-3$, respectively, corresponding to the surface plot truncations of Fig. 3. Otherwise, they would become progressively smaller and closer together until they converged to the point $R|_{x=L}=\sqrt{2}/2+j\sqrt{2}/2$. This point and the divergence pair rotate counterclockwise around the unit circle with increasing frequency.

Further inspection of these figures and Eqs. (25) and (26) reveals that as long as $|R|_{x=L}<1$, any value of $R|_{x=L}$ yields a value of $I/I_{an}>0$; net sound-energy flux is directed toward the termination for all values of kL so that the vibrating piston consistently absorbs at least a portion of the steady-state incident intensity. Interestingly, if $R|_{x=L}$ is held constant in this range, the frequency-averaged total intensity (averaged over integer multiples of kL/π or over an interminably wide bandwidth) remains identical to that encountered under the anechoic boundary condition. In contrast, if $|R|_{x=L}>1$, total sound-energy flux is consistently directed away from the termination, toward the enclosed sound field and the primary piston. If $R|_{x=L}$ is held constant in this range, the frequency-averaged total intensity is equal in magnitude, but opposite in direction to that present under the anechoic boundary condition.

As $|R|_{x=L}\rightarrow 1$, the total intensity ratio in Eq. (26) converges to zero for most kL, but periodically diverges with dependence upon complex $R|_{x=L}$. When $R|_{x=L}$ is held constant with a modulus of unity, the frequency-averaged intensity ratio tends to zero. The behavior of the reflected intensity ratio in Eq. (27) also depends upon complex $R|_{x=L}$ as $|R|_{x=L}\rightarrow 1$. If the coefficient contains an imaginary component, the ratio diverges periodically over kL. However, if the coefficient is purely real, it coincides with a rigid surface which must produce a ratio of unity.

An examination of total acoustic energy within the enclosure reveals further differences between the two-piston and semi-infinite plane wave tube models. Equations (10) and (15) yield the following relationship for total energy:

$$E=\frac{\rho_0 SL}{2}|\hat{u}_1|^2\left\{\frac{|R|^2_{x=L}+1}{|R|^2_{x=L}+1-2[(R_R|_{x=L})\cos 2kL+(R_I|_{x=L})\sin 2kL]}\right\}. \tag{28}$$

The ratios of total energy with arbitrary $R|_{x=L}$ to the total energies present under anechoic and rigid boundary conditions are then

$$\frac{E}{E_{an}}=\frac{|R|^2_{x=L}+1}{|R|^2_{x=L}+1-2[(R_R|_{x=L})\cos 2kL+(R_I|_{x=L})\sin 2kL]}, \tag{29}$$

$$\frac{E}{E_{rg}}=\frac{2\sin^2 kL(|R|^2_{x=L}+1)}{|R|^2_{x=L}+1-2[(R_R|_{x=L})\cos 2kL+(R_I|_{x=L})\sin 2kL]}. \tag{30}$$

In the limit of large $R|_{x=L}$, i.e., for $|R|_{x=L}\gg 1$, the ratio in Eq. (29) tends to unity. Thus, the total acoustic energy in the enclosure approaches that present under the anechoic boundary condition; there is no significant increase. One example of such behavior is mentioned in Sec. III A, wherein the termination is controlled to eliminate steady-state pressure incident upon it. Under this condition, the reflection coefficient modulus at the termination tends to infinity for all values of kL, except as $kL\rightarrow n\pi$. The termination velocity is adjusted relative to the primary source velocity in a manner that effectively causes the primary source to behave as an anechoic absorber. The total energy is therefore equal to that of the complementary condition in which the termination acts as the anechoic absorber. In addition, it is clear from Eq. (29) that for $|R|_{x=L}\ll 1$, total energy in the enclosure consistently approaches that present under the anechoic condition. Hence, large relative changes (either increases or decreases) in total enclosed energy occur only when the termination reflection coefficient modulus roughly approaches unity. Some of the control examples discussed in Sec. III B are representative of this behavior for energy decreases.

Enclosed energy characteristics are further clarified in Fig. 5. A surface plot of the energy ratio E/E_{an} is shown for

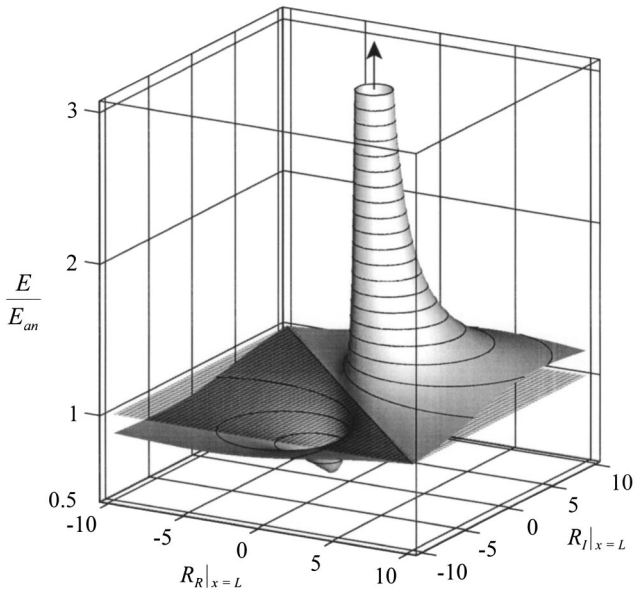

FIG. 5. Surface plot showing the ratio of total energy in the two-piston plane wave tube to that present under an anechoic termination condition. The ratio is plotted as a function of the real and imaginary parts of the termination reflection coefficient, $R_R|_{x=L}$ and $R_I|_{x=L}$, for $f=9c/16L$. Contour lines are shown at increments of 0.1. The superposed mesh represents the $E/E_{an}=1$ plane.

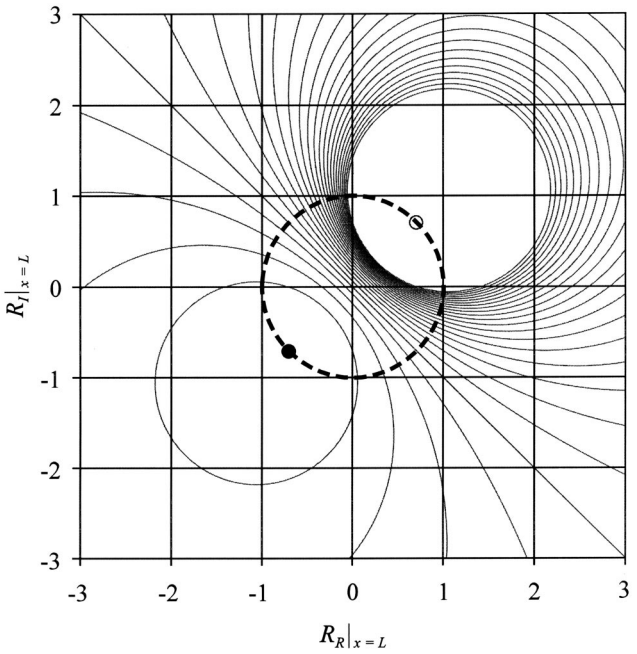

FIG. 6. Contour plot showing the ratio of total energy in the two-piston plane wave tube to that present under an anechoic termination condition. The ratio is plotted as a function of the real and imaginary parts of the termination reflection coefficient, $R_R|_{x=L}$ and $R_I|_{x=L}$, for $f=9c/16L$. Contour lines are shown at increments of 0.1 with truncation at $E/E_{an}=3$ (see Fig. 5). The heavy dashed circle delineates $|R|_{x=L}=1$. The small ring on the unit circle marks the point of maximum divergence, whereas the small black dot marks the point of the ratio minimum ($E/E_{an}=0.5$).

the frequency $f=9c/16L$ with a superposed mesh representing the $E/E_{an}=1$ plane. The rise between consecutive contour lines again represents a ratio increment of 0.1. The plot shows that the ratio diverges around one point on the complex $R|_{x=L}$ plane and converges to a minimum value of 0.5 at another. At several other points, including those for which $|R|_{x=L}\gg 1$, it approaches a value of 1. Figure 6 provides additional insight through a closer overhead view of the contours. The eccentric rings accumulating in the divergent region of the upper-right quadrant are truncated at $E/E_{an}=3$ to correspond to the surface plot truncation of Fig. 5. Otherwise, they would become progressively smaller and closer together until they converged to a single point encircled by the small ring on the unit circle: $R|_{x=L}=\sqrt{2}/2+j\sqrt{2}/2$. The eccentric rings accumulating less conspicuously in the lower-left quadrant correspond to the ratio minimum of 0.5. The inner-most contour ring shown for the region has a value of $E/E_{an}=0.6$. With finer contour increments, additional rings would become apparent that converge to the minimum point indicated by the black dot on the unit circle: $R|_{x=L}=-\sqrt{2}/2-j\sqrt{2}/2$. Accordingly, both the point of divergence and the ratio minimum fall on the $|R|_{x=L}=1$ circle, 180 degrees from each other. This pair rotates counterclockwise around the circle with increasing frequency.

It is important to recognize that under some conditions, reflection coefficients with moduli less than unity, i.e., $|R|_{x=L}<1$, can relatively increase total energy in the enclosed field. Purely real reflection coefficients in the range $0<R_R|_{x=L}<1$ increase energy relative to that encountered under the anechoic boundary condition but not relative to that encountered under the rigid boundary condition. However, purely imaginary or complex reflection coefficients, even with very small imaginary components in the range $0<R_I|_{x=L}<1$, can produce significant increases to total energy in comparison to that encountered under *either* benchmark condition. As these imaginary components become larger within this range, the increases may become particularly dramatic, even when averaged over frequency.

With these developments in mind, it is instructive to revisit the past interpretations for $|R|>1$ mentioned in the introduction—each coming from studies involving physical arrangements similar to the two-piston plane wave tube model.[29] It is clear from the present results that such large reflection coefficient moduli do *not* necessarily connote (1) an increase in an intensity quantity or (2) an addition of energy to the field in comparison to that encountered under anechoic or rigid benchmark conditions. While it is true that sound-energy flux is directed toward the adjacent field for $|R|>1$, energy is not supplied to the field in the sense that it necessarily *augments or maintains* the field energy relative to a benchmark condition. In essence, direction of flux is extraneous to the total enclosed energy. In some cases, values of $|R|>1$ relatively *diminish* total enclosed energy, whereas in other cases, values of $|R|<1$ relatively *increase* total enclosed energy. Furthermore, neither sound-energy flux nor total enclosed energy is generally proportional to $|R|$ or $|R|^2$. In fact, the analysis indicates that the most dramatic swings in these quantities occur as $|R|\to 1$. Thus, the concept of $|R|>1$ connoting a supply of energy to the adjacent field loses relevance. The interpretation that $|R|>1$ connotes a super-reflection that increases reverberation within the adjacent sound field does not generally hold if the term ''super-reflection'' describes reflected intensity magnitude exceeding that reflected from a rigid termination. However, if it describes reflected intensity magnitude exceeding incident intensity magnitude, the discussion in Sec. III A suggests that the concept does hold. Nevertheless, the total steady-state energy in the enclosure, which involves reflected energy, certainly does *not* always increase for values of $|R|>1$.

V. CONCLUSIONS

This work has demonstrated that reflection coefficients of active boundary surfaces and their effects on adjacent one-dimensional sound fields may be misinterpreted when important physical properties of the systems are overlooked. In the past, conclusions about these surfaces have coincided ostensibly with constant incident pressure models and behaviors of passive materials. This analysis has demonstrated several distinctions that broaden understanding of the surfaces and their potentially large reflection coefficients (i.e., $|R|>1$).

Investigation of a finite-length plane wave tube with a primary piston source and an active piston termination has produced several important results that clarify relationships between reflection coefficients and pertinent time-averaged energy quantities. First, for the active termination to create a value of $|R|$ greater or less than unity, or to allow a net flow of sound energy, its velocity must have an imaginary component relative to that of the primary source. Second, to understand the impact of reflection coefficients upon energy

flux or total enclosed energy in the tube, one must not only know the reflection coefficient modulus at the termination, but its real and imaginary components. Third, increases in reflection coefficient moduli at the termination *do not* necessarily indicate corresponding increases in sound-energy flux back toward the enclosed space or total enclosed energy. Fourth, energy-related effects of reflection coefficient moduli at the termination are frequency-dependent functions of the adjacent space and vibration of the primary source. Fifth, while reflection coefficient moduli exceeding unity may not produce *absorption* of energy at the termination, they can relatively *reduce* the vector magnitude of total intensity and total energy within the enclosed space. Sixth, very large reflection coefficients (i.e., $|R| \gg 1$), produce both a vector magnitude of total intensity and total enclosed energy approaching those present under an anechoic boundary condition (i.e., $|R| = 0$). Seventh, large relative changes (either increases or decreases) in total intensity and total enclosed energy occur only as active termination reflection coefficient moduli roughly approach unity.

From these findings one may conclude that sound-energy-related effects of active boundary surfaces are frequency-dependent functions of the spaces they bound and the acoustic field generated by one or more additional sources operating within the same spaces. One may not generally conclude that active boundary surfaces operating with given reflection coefficient moduli in one space or with certain interacting sources necessarily produce the same energy-related effects in another space or with dissimilar interacting sources or source positions. Because active boundary surfaces are secondary sources that interact with other sources, relationships between their reflection coefficient moduli and energy-related effects in adjacent fields are not necessarily straightforward. Further analysis is required to develop additional relationships and more extensive understanding for three-dimensional systems.

[1] H. F. Olson and E. G. May, ''Electronic sound absorber,'' J. Acoust. Soc. Am. **25**, 1130–1136 (1953).

[2] H. F. Olson, ''Electronic control of noise, vibration, and reverberation,'' J. Acoust. Soc. Am. **28**, 966–972 (1956).

[3] D. Guicking and K. Karcher, ''Active impedance control for one-dimensional sound,'' J. Vibr. Acoust. **106**, 393–396 (1984).

[4] D. Guicking and M. Albrecht, ''An electret loudspeaker for active acoustic systems,'' J. Vibr. Acoust. **106**, 397–398 (1984).

[5] D. Guicking, K. Karcher, and M. Rollwage, ''Coherent active methods for applications in room acoustics,'' J. Acoust. Soc. Am. **78**, 1426–1434 (1985).

[6] T. Yagi, A. Imai, and M. Konishi, ''Variable sound absorption system using velocity and pressure feedback loudspeaker,'' Proceedings of the International Symposium on Active Control of Sound and Vibration, Tokyo, Japan, 1991, pp. 433–438.

[7] P. Darlington and G. C. Nicholson, ''Theoretical and practical constraints on the implementation of active acoustic boundary elements,'' Proceedings of the Second International Congress on Recent Developments in Air- and Structure-Borne Sound and Vibration, Auburn, Alabama, USA, 1992, pp. 1011–1018.

[8] F. Orduña-Bustamante and P. A. Nelson, ''An adaptive controller for the active absorption of sound,'' J. Acoust. Soc. Am. **91**, 2740–2747 (1992).

[9] C. R. Fuller, M. J. Bronzel, C. A. Gentry, and D. E. Whittington, ''Control of sound radiation/reflection with adaptive foams,'' Proceedings of Noise-Control 94, Ft. Lauderdale, Florida, USA, 1994, pp. 429–436.

[10] R. L. Clark and D. G. Cole, ''Active damping of enclosed sound fields through direct rate feedback control,'' J. Acoust. Soc. Am. **97**, 1710–1716 (1995).

[11] X. Meynial, ''Active materials for applications in room acoustics,'' Proceedings of the Third International Conference on Intelligent Materials, Lyon, France, 1996, pp. 968–973.

[12] P. Darlington and M. R. Avis, ''Noise control in resonant soundfields using active absorbers,'' Proceedings of Inter-Noise 96, Liverpool, England, 1996, pp. 1121–1126.

[13] P. Darlington, ''Active boundary control of enclosed sound fields,'' Proceedings of Inter-Noise 96, Liverpool, England, 1996, pp. 1127–1132.

[14] T. W. Leishman, ''Active control of sound transmission through partitions composed of discretely controlled modules,'' Ph.D. thesis, The Pennsylvania State University, University Park, Pennsylvania, USA, 2000.

[15] P. M. Morse and K. U. Ingard, *Theoretical Acoustics* (Princeton University Press, Princeton, NJ, 1968), pp. 375–376.

[16] In this paper, **boldface type** indicates vector quantities. The symbol $\mathbf{e}_x$ denotes a unit vector in the direction of increasing x. Superimposed circumflex marks ($\wedge$) indicate complex frequency domain amplitudes of acoustic or mechanical signals.

[17] F. J. Fahy, *Sound Intensity*, 2nd ed. (E&FN Spon, London, 1995).

[18] L. G. Beatty, ''Acoustic impedance in a rigid-walled cylindrical sound channel terminated at both ends with active transducers,'' J. Acoust. Soc. Am. **36**, 1081–1089 (1964).

[19] W. L. Rogers, ''Experiments using an active duct termination to control acoustic impedance,'' ASHRAE Trans. **79**, Pt. 2, 167–171 (1973).

[20] A. R. D. Curtis, P. A. Nelson, S. J. Elliott, and A. J. Bullmore, ''Active suppression of acoustic resonance,'' J. Acoust. Soc. Am. **81**, 624–631 (1987).

[21] P. A. Nelson and S. J. Elliott, *Active Control of Sound* (Academic, London, 1992).

[22] W. S. Kim and M. G. Prasad, ''Acoustic impedance of a finite length duct with dynamic termination,'' J. Acoust. Soc. Am. **91**, 3575–3578 (1992).

[23] D. Thenail, O. Lacour, M. A. Galland, and M. Furstoss, ''The active control of wall impedance,'' Acustica **83**, 1039–1044 (1997).

[24] Notice that the velocity sense of piston 2 is opposite that of piston 1 and that of the semi-infinite tube termination. Both pistons in this model are assumed to radiate *into* the enclosed medium, creating an adjacent local fluid compression with positive piston displacement.

[25] C. H. Hansen and S. D. Snyder, *Active Control of Noise and Vibration* (E&FN Spon, London, 1997).

[26] S. D. Sommerfeldt and P. J. Nashif, ''An adaptive filtered-x algorithm for energy-based active control,'' J. Acoust. Soc. Am. **96**, 300–306 (1994).

[27] J. W. Parkins, S. D. Sommerfeldt, and J. Tichy, ''Narrowband and broadband active control in an enclosure using the acoustic energy density,'' J. Acoust. Soc. Am. **108**, 192–203 (2000).

[28] Although the reflection coefficient modulus is uniform along the length of the lossless plane wave tube, the representation $|R|_{x=L}$ is used for consistency with the complex $R|_{x=L}$ that must be evaluated at the termination.

[29] The primary and secondary sources used in the studies were ostensibly transducers of finite internal impedance. In one instance (Ref. 11), a layer of absorptive material was positioned in the tube near the primary source.